Int J Adv Manuf Technol (2011) 54:567–578
DOI 10.1007/s00170-010-2953-3

ORIGINAL ARTICLE

Investigation of micro-milling process parameters for surface roughness and milling depth

Ibrahim Etem Saklakoglu · Sefika Kasman

Received: 23 March 2010 / Accepted: 21 September 2010 / Published online: 12 October 2010

Abstract The main objective of this study is to investigate the micro-milling performance of the AISI H13 with different process parameters namely laser power, scan speed, frequency, and fill spacing using 30W fiber laser marking machine and to find the optimal operation conditions for minimum surface roughness and maximum milling depth. The 108 different combinations occurred with the interaction of each level of the parameters used in this study. Therefore, the main contribution of this paper to the related literature is that it produces new evidence regarding the effects of the multi-scan times on both surface roughness and milling depth. The experimental results are showed that 0.03 mm of fill spacing, the highest scan speed (800 mm/s), lowest frequency (20 kHz), and laser power (60%) produced better surface roughness, which is 1.75 μm. The deeper cavity on the geometry is obtained under the experimental combination as 200 mm/s of scan speed, 0.02 mm of fill spacing, 60% of laser power, and 40 kHz of frequency, which is 195 μm. The regression analysis was used to develop a mathematical model and determine the effect of process parameters on the surface roughness and milling depth. The results of subsequent tests verifies regression models.

I. E. Saklakoglu (✉)
Faculty of Engineering, Department of Mechanical Engineering,
Ege University,
Izmir, Turkey
e-mail: i.e.saklakoglu@ege.edu.tr

S. Kasman
Department of Technical Program, Izmir Vocational School,
Dokuz Eylul University,
Izmir, Turkey

Keywords Laser micro-milling · Surface roughness · Milling depth · Fiber laser

1 Introduction

Laser-assisted applications for micro-machining process includes ablation, engraving, drilling, cutting, marking, and milling which are used in many industrial applications such as semiconductor, electronics, medical, automotive, aerospace, instrumentation, and communications [1, 2]. The industrial lasers for micro-processing are used to solve the challenges of complex and smaller geometry requirements. It is well-known that the small features on the geometry are requires precise tool action and tool geometry. The conventional micro-milling processes use a cutting tool to mechanically cut the material to achieve the desired geometry, but the tool geometry and actions have major effects on the results of the process. Laser micro-milling provides many machining solutions compared with the conventional process due to the non-contact process [1–5]. Laser-assisted machining application eliminates tool-based problems [1, 6]. Therefore, the effect of vibrations and cutting forces does not occur on the machined surface [1].

Laser micro-milling technique is the thermal machining process [1, 2] which is used to remove material through the reaction between the laser beam and the workpiece. A high intensity focused laser beam moves over the geometry and creates a thermal reaction in the interaction zone with metal. Due to this reaction, the sufficient material in the interaction zone is melted or evaporated [2, 3]. The removal mechanism occurs in layers [5, 7]. The thickness of removed layer in every time and substrate surface roughness is controlled by energy density.

Table 1 Chemical composition of AISI H13

C	Cr	Mn	Mo	V	Si	Fe
0.3%	5.54%	0.36%	1.33%	0.4%	1%	Bal.

There are lots of factors of process control, but generally the combinations of more than one factor have major effect on both energy density and heat input. The main factors used in the micro-milling by laser are laser power, scan speed, frequency, fill spacing, and scan direction strategy.

Laser micro-milling technique is commonly used for engraving of complex shaped parts, hard materials, and difficult to machine with conventional techniques. The material used in this study is a hot work tool steel (AISI H13). This material is most widely used in making molds for micro-injection and extrusion and dies for stamping and forging. The grade AISI H13 is difficult to machine by conventional process due to complex geometry.

The main aim of this study is to investigate the machinability of AISI H13 by fiber laser and to evaluate the effect of process parameters on the machining results using full factorial design and regression analyzes. There are many studies related to the laser-based machining methods. However, there were not observed similar studies in the literature for micro-machining of AISI H13 using 30-W fiber laser. Many theoretical, analytical, and experimental works using the laser-based machining techniques have been studied and researcher concentrated on machining performance of both laser system and parameters.

Laser milling techniques is one of the attractive and new method in the micro-processing of parts, which is being used in biomedical, electronic, computer, and mold having complex shapes. The advantages of laser milling technique such as saving cost and time, dimensional accuracy, and machining without cutting tool has drawn the attention of researchers. The purpose is to produce precision parts and to develop an alternative method against the conventional technique to solve the machining problem. In the laser-based machining literature, all of milling studies were performed on engraving, erosion, and marking. Most of the studies were performed in order to determine the effect of the process parameters on the surface roughness, ablation depth, and mark contrast. In these studies, the CO_2 and Nd:YAG lasers were mostly used. Some selected studies are presented which are: Leone et al. [3] studied marking tests on AISI 304 SS steel using a Q-switched diode-pumped Nd:YAG laser, in order to determine the best working parameters to obtain a visibility. They found that both mark with and mark visibility is affected by operating conditions. Also, they showed that the surface roughness and oxidation plays role on the mark contrast. Leone et al. [4] studied to investigate the influence of the process parameters (multiple laser scanning, varying the pulse frequency, the scanning speed, and the number of scanning repetitions) on the material removal rates by engraving panels made of different types of wood using a Q-switched diode-pumped Nd:YAG green laser working with a wavelength λ= 532 nm. They found that the engraved depth is strongly affected by the mean power, the pulse frequency, the beam speed, and the number of repetitions. Yasa et al. [5] worked on selective laser erosion of AISI 1045 steel. In their studies, they were able to determine the effect of process parameters on the surface roughness and depth per layer using Nd:YAG laser source. It is reported that the factors which scan overlap, pulse overlap, and laser parameters (scan speed, laser power, frequency, and scan strategy) have significant effect on the minimum surface roughness and depth per layer. Campanelli et al. [7] used the design of experiments to investigate the effect of process parameters (scan speed, frequency, power, overlapping, and scan strategy) on the surface roughness and the depth of removed material using factorial analyze. All tests were conducted on aluminum–magnesium alloy specimens using a laser marker machine equipped with a pulsed Nd:YVO4. Wendland et al. [8] investigated deep engraving of aluminum grade 5251 and stainless steel grade 316 using Nd:YAG laser source. They investigated high removal rates and surface modification at different process condition. It is concluded that the factor used in the experiments affect the surface roughness and removal rates. Qi et al. [9] investigated the effect of process parameters (pulse frequency, electric current, and scanning speed) on mark the depth, width, and contrast using a Q-switched Nd:YAG laser. They found that the mark depth, width, and contrast interaction between material and laser beam, which was influenced by frequency.

Table 3 Laser milling parameters

Symbol	Parameters	Levels
P	Laser power (W), (%)	60, 80, 100
SS	Scan speed (mm/s)	200, 400, 600, 800
F	Frequency (kHz)	20, 30, 40
FS	Fill spacing (mm)	0.02, 0.03, 0.04

Table 2 Mass volume ρ, calorimetric capacity C, conductivity K, and latent melting energy L_f at fusion temperature T_f

T_f (°C)	ρ (kg m^{-3})	C (J kg^{-1} K^{-1})	K (Jm^{-1} s^{-1} K^{-1})	L_f (J kg^{-1})
1,500	7,000	657	25	247

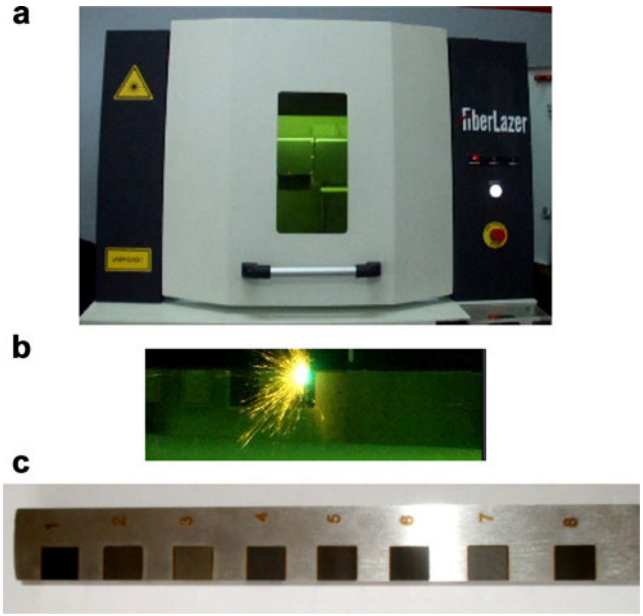

Fig. 1 The machined sample and fiber laser machine used for experiments; **a** is the fiber laser machine, **b** is the machined surface, **c** is the machined sample

The published papers in the related literature are subjected of the effect of process parameters on the surface roughness and depth. The lasers used in the experiments are CO_2 and Nd:YAG. The laser used in this study is 30W fiber laser and also, the fiber laser has been receiving attention due to its advantages of high power, beam quality, simplicity, high electrical and optical efficiency, reliability, excellent thermal properties, and running cost [14]. Due to difference of laser system, process outputs, values of parameters, and workpiece material when compared to present studies show variation. And the researchers have ignored the effect of multi-scan times on their studies. Therefore, the main contribution of this paper to the related literature is that it produces new evidence regarding the effects of the multi-scan times on both surface roughness and milling depth.

This paper presents an experimental and a statistical study relating to the investigation of the correlation between process parameters and process responses. The study was evaluated at two stages. Firstly, the experimental studies were analyzed using full factorial method and after that, an analysis of the variance (ANOVA) analysis and a linear regression model was constituted to find out which parameters have significant effect on the responses of the process and to conduct a mathematical model, respectively. The evaluated process responses are the surface roughness (SR) and the milling depth (*Dm*).

Factorial experiments explain the effect of process having large number of independent variables on the response. In determining the process parameters combined with different level for minimum surface roughness and maximum depth, the full factorial design matrix was constituted in this study. The main aim of using the factorial experiment and regression analyze is to detect the effect of each parameter and interaction with each other on the responses and to explain the effects as a numeric value using a mathematical model developed results of experiments. The current results taken from experiments aim to understand the effect of main parameters of laser-based micro-milling process of AISI H13 and to create a

Table 4 The ANOVA table of mean for the SR based on the full factorial design

Source	DF	SS	MS	*F*	*P*	Percentage of contribution
P	2	559.62	279.809	381.25	0.000	16.62
F	2	19.71	9.856	13.43	0.000	0.585
SS	3	2,024.50	674.834	919.50	0.000	60.12
FS	2	45.55	22.775	31.03	0.000	1.35
P×*F*	4	83.52	20.879	28.45	0.000	2.48
P×SS	6	466.61	77.769	105.96	0.000	13.86
P×FS	4	18.02	4.506	6.14	0.002	0.535
F×SS	6	48.56	8.093	11.03	0.000	1.44
F×FS	4	2.15	0.537	0.73	0.579	0.064
SS×FS	6	22.89	3.815	5.20	0.001	0.68
P×*F*×SS	12	10.20	0.850	1.16	0.364	0.303
P×*F*×FS	8	17.32	2.16	2.95	0.019	0.514
P×SS×FS	12	21.26	1.77	2.41	0.032	0.63
F×SS×FS	12	9.71	0.81	1.10	0.402	0.29
Residual error	24	17.61	0.734			0.527
Total	107	3,367.22				100

Table 5 The ANOVA for the Dm based on the full factorial design

Source	DF	SS	MS	*F*	*P*	Percentage of contribution
P	2	39,673	19,836.6	261.61	0.000	20.758
F	2	863	431.5	5.80	0.009	0.452
SS	3	98,048.4	32,682.8	439.27	0.000	51.30
FS	2	16,139	8,069.7	108.46	0.000	8.44
P×*F*	4	3,966.6	991.7	13.33	0.000	2.075
P×SS	6	15,224.8	2,537.5	34.10	0.000	7.966
P×FS	4	629.4	157.3	2.11	0.110	0.330
F×SS	6	2,570.5	428.4	5.76	0.001	1.345
F×FS	4	571.8	142.9	1.92	0.139	0.299
SS×FS	6	1,015.2	169.2	2.27	0.07	0.531
P×*F*×SS	12	7,783.6	648.6	8.72	0.000	4.072
P×*F*×FS	8	231.3	28.9	0.39	0.916	0.121
P×SS×FS	12	1,975.2	164.6	2.21	0.047	1.033
F×SS×FS	12	640.6	53.4	0.72	0.721	0.335
Residual error	24	1,785.6	74.4			0.934
Total	107	191,118.6				100

process map for researcher or producer. In this regard, the present research is an original study and will contribute to the related literature with the results obtained large experimental studies.

2 Experimental works

Laser micro-milling process was performed in order to achieve deep cavity on the workpiece surface. Therefore, the experiments were implemented to obtain the best process performance. Two different process performances namely surface roughness (SR) and milling depth of geometry (Dm) were investigated.

2.1 Material

The hot work tool steel grade AISI H13 was used in the experimental works. Its chemical composition and physical properties are given in Tables 1 and 2, respectively. The workpiece was made up a rectangular plate with a dimension in 20×150×20 mm.

2.2 Micro-milling process

The laser micro-milling experiments were performed by laser marking machine equipped with a ytterbium-doped fiber laser having a wavelength of 1,064 nm. Maximum output power is 30 W. In the machine system software, the laser power is input as a percentage of the maximum laser power. During the experiments, the laser beam was focused onto the workpiece surface at a 175 mm focal length which yields a laser spot diameter of about 100 μm. The selected geometry for experiments was a square with dimension of 10×10 mm. The motion of the laser beam and the process parameters were controlled by a PC and software. The micro-milling test sample was stationary and mounted on an aluminum plate. Each machining area was scanned 20 times at the parallel scanning direction (0°) to achieve deep cavity result. All of the experiments were performed in the standard atmospheric conditions and no assist gas was used. The surface of the test samples were machined as a function of the process parameters, which is given in Table 3. Figure 1 shows the machined sample and fiber laser machine used for experiments.

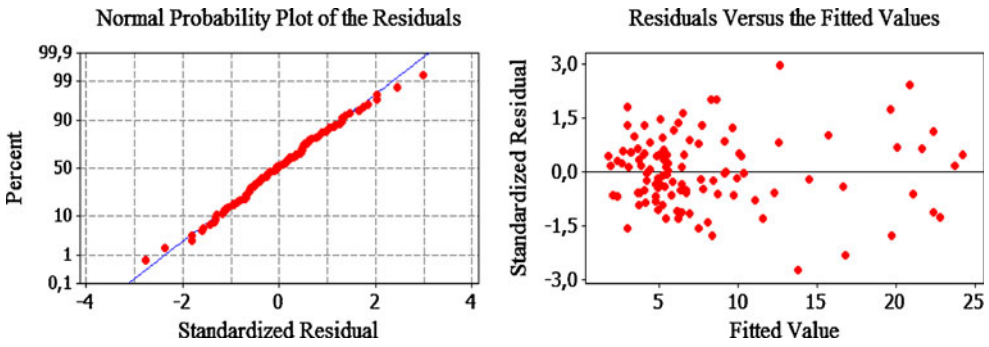

Fig. 2 Normal probability and residuals based on full factorial analyze plots for the means of SR

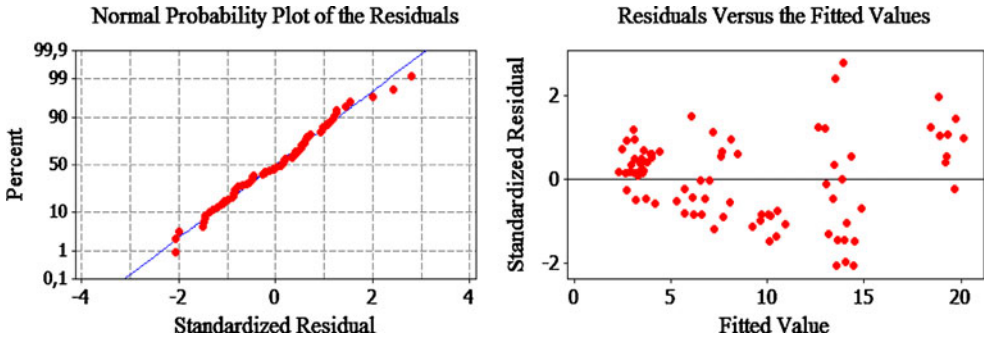

Fig. 3 Normal probability and residuals plots based on regression model for the means of SR

2.3 Selection of micro-milling parameters and experimental procedure

The milling depth and the surface roughness of machined geometry are changed as a function of the workpiece material and process parameters. Previous works showed that four main parameters play important role on the depth and surface roughness in the micro-milling process. These are the laser power, scan speed, frequency, and fill spacing. The selected values of process parameters are given in Table 3. Using the full factorial experimental design, 108 different experimental conditions were constituted in order to investigate the effects of process parameters on the SR and Dm. In addition to the factorial analysis, the mathematical relations were developed using regression analysis in order to express the relations between the responses and the four parameters. The relations were based on the results of data obtained from these 108 experiments.

2.4 Analysis of experiments

All combinations created according to the full factorial experimental design were experimented and results for SR and *Dm* were evaluated using ANOVA. The result of ANOVA consists the degrees of freedom, the sequential sum of squares (Seq SS), the adjusted sum of squares (adj SS) and the adjusted mean squares (adj MS), and *F* and *P* values. The analysis was carried out at 5% significant level and 95% confidence level. In analyses, *F* value is the mean square error to residual and is used to determine the significance of a factor. *P* value reports the significance level. The last column of the table shows the percentage value of each parameter contribution (ρ) which indicates the degree of influence on the process performance.

The parameters and their possible interactions have a significance on the SR and *Dm* was used to create a mathematical model using regression analysis. The ANOVA results taken from the regression model were used to determine the significance of the regression model.

2.5 Measurements

In this study, the Dm and the Ra are evaluated as the performance and outputs of the process. A Mitutoya SJ-301 model profilometer was used to analyze the Dm and the Ra. The parameter "Ra" were used to determine the surface

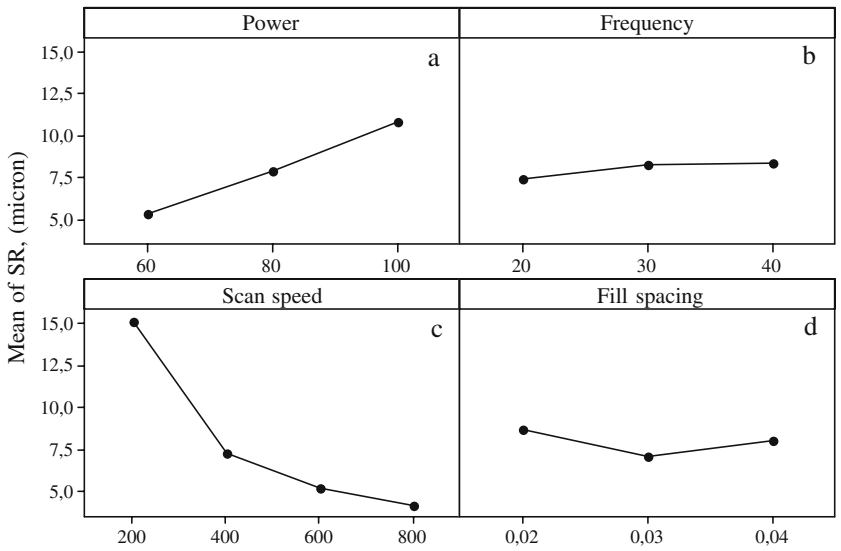

Fig. 4 Main effects plot based on the full factorial design for the means of SR

Table 6 Predicted levels of parameters for the minimum SR and the maximum Dm using highest S/N ratio

Optimal level of parameters	S/N ratio predicted
SR	$P_1F_1SS_4FS_2$
Dm	$P_3F_3SS_1FS_1$

roughness. The average roughness (Ra) is the arithmetic mean of absolute values of profile deviations (Y_i) from the mean line. The parameter "Ry" were used to determine the Dm. Ry is the sum of height Yp of the highest peak from the mean line and depth Yv of the deepest valley from the mean line. Measurements for Ra and Dm were performed in cut off length of 0.8 mm, sampling length of 5 mm, and traversing speed of 0.5 mm/s. All of the measurements for Ra and Dm were replicated five times to provide the statistical accuracy. The average of those measured five values was calculated and used as a final value. The measured values were recorded as μm.

3 Results

As mentioned above, four parameters were selected for investigation of micro-milling process and these were studied at mixed level. The experiments were conducted using full factorial design.

3.1 Analysis results for SR and Dm

Tables 4 and 5 show the ANOVA results of mean for SR and Dm based on the full factorial design. Table 4 shows the results of ANOVA for SR indicate that except from the two-way interaction, that is *F*×FS, and three-way interactions, these are *P*×*F*×FS and *F*×SS×FS, all remaining parameters and interactions significantly affect the SR since the probability values were lower than 0.05. The highest percentage contribution for SR was observed at scan speed, which is 60.12%. The other highest percentage contributions were observed at *P* and *P*×PS, the values are 16.62% and 13.86%, respectively. Even though some of the two- and three-way interactions have a significant effect, their contributions on the SR are small enough to be neglected.

The normal plot of residuals is used to test the normal distribution of data [15]. The residual is the difference between the observed and predicted value from the regression. If the points on the plot are the fairly close to the straight line, it means that the data are normally distributed [16]. The normal plot of residuals and residuals versus the fitted values based on the full factorial analysis and regression model for the SR is shown in Figs. 2 and 3. The plot shows that there is a linear distribution and which means that the residuals having a normal distribution. The plot of residual versus fitted values for SR indicates that the residuals values are distributed normally with a constant variance.

Figure 4 shows the main effects of SR plot, which is used to predict the optimum levels of the process parameters for minimum SR. According to Fig. 4, the predicted optimal SR value is the P1F1SS4FS2, which is reported in Table 6.

Table 5 shows the results of ANOVA for Dm indicate that the two-way interaction that is *P*×FS, *F*×FS, and SS×FS and almost all three-way interactions have insignificant effect and all of main and remaining interactions significantly affect the Dm since the probability values were lower than 0.05. The parameters having highest percentage contribution for Dm are scan speed, power, and fill spacing and their contributions are 51.30%, 20.758%, and 8.44%, respectively.

The normal plot of residuals and the residuals versus the fitted value plot based on the full factorial analysis and regression model for the Dm is shown in Figs. 5 and 6. It can be seen from the Fig. 5 where the distribution of residuals shows nearly linear trend and residuals are normally distributed.

Figure 7 shows the main effects of Dm plot, which is used to predict the optimum levels of the process parameters for maximum milling depth. According to Fig. 7, the predicted optimal milling depth value is the P3F3SS1FS1, which is reported in Table 6.

3.2 Development of a mathematical model using regression analysis

After experimental analysis of factor effects, the main effects of laser power, frequency, scan speed, and fill spacing and the

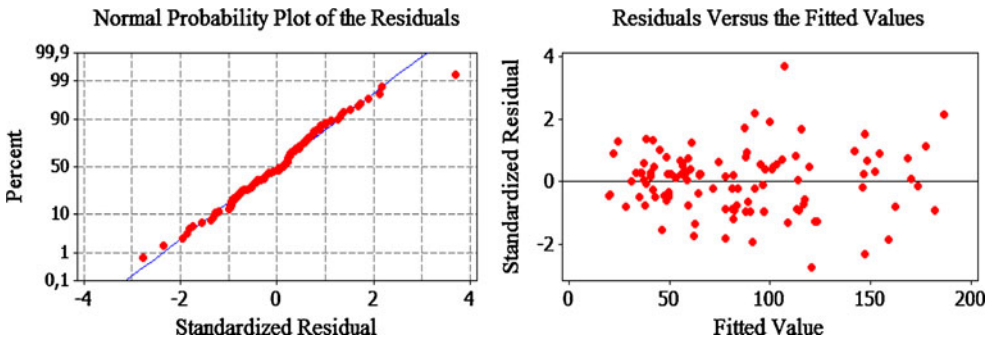

Fig. 5 Normal probability and residuals based on full factorial analyze plots for the means of Dm

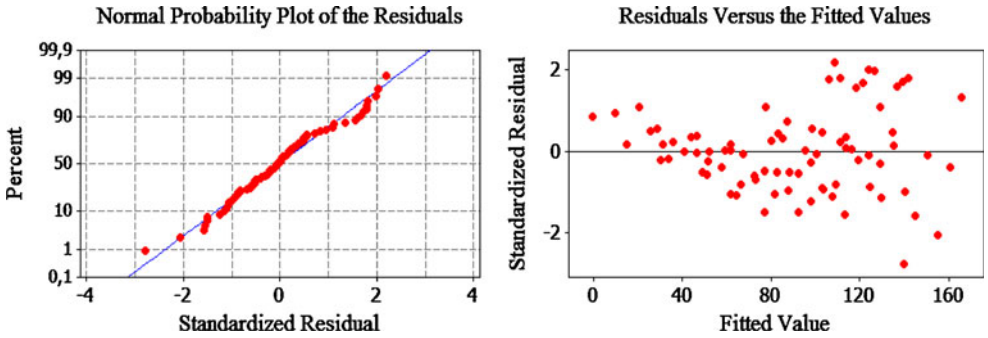

Fig. 6 Normal probability and residuals plots based on regression model for the means of Dm

interactions having significant effect on the responses used to establish a mathematical model. A statistical ANOVA is employed to determine the significance of mathematical model taken from regression analysis. To characterize the surface roughness and depth of machined area, two second-order regression models were constituted. The scan speed of 600 mm/s used in factorial analysis was not used in regression analysis. The data used to control of regression model. The estimated regression equations are given in Eqs. 1 and 2.

$$\mathrm{SR} = -13.8970 + 0.3858 \times P + 0.0397 \times F + 0.0206 \times \mathrm{SS} - 45.3704 \times \mathrm{FS} - 0.0005 \times P \times \mathrm{SS} \quad (1)$$

$$\mathrm{Dm} = 103.73 + 1.05 \times P + 0.25 \times F - 0.13 \times \mathrm{SS} - 1,540.15 \times \mathrm{FS} \quad (2)$$

Table 7 shows the estimated coefficient and significance of coefficient of the variables for SR model. The table indicates that except the frequency (F) and fill spacing (FS), other main parameters and interaction are significant at the 0.05 level since their P values are lower than 0.05. The same analysis was performed for Dm. Table 8 shows the estimated coefficient and significance of coefficient of the variables for Dm model. It can be seen from the P values that except the frequency, all main parameters and interactions are significant at 0.05 level. The validity of two models is analyzed by using the ANOVA. The results for SR and Dm are reported in the Tables 9 and 10, respectively. The P values are 0.000 for two responses and which indicated that the estimated regression model is significant at the 0.05.

In order to test validity and verify of the regression models, a few confirmation tests were conducted on the workpiece. Therefore, one measurement for SR was found from the regression equation and the related measurement for SR was also found from the experimental trials. The results are reported in Table 11. The predicted values for SR were calculated with the equation of the regression model while the experimental values were measured during the experimental trials. The same process is also used for the Dm and results reported in Table 12. In order to determine the accuracy of the predicted regression model, the percentage prediction error was calculated for all test conditions. The results of percentage prediction error for SR and Dm are reported in Tables 11 and 12, respectively.

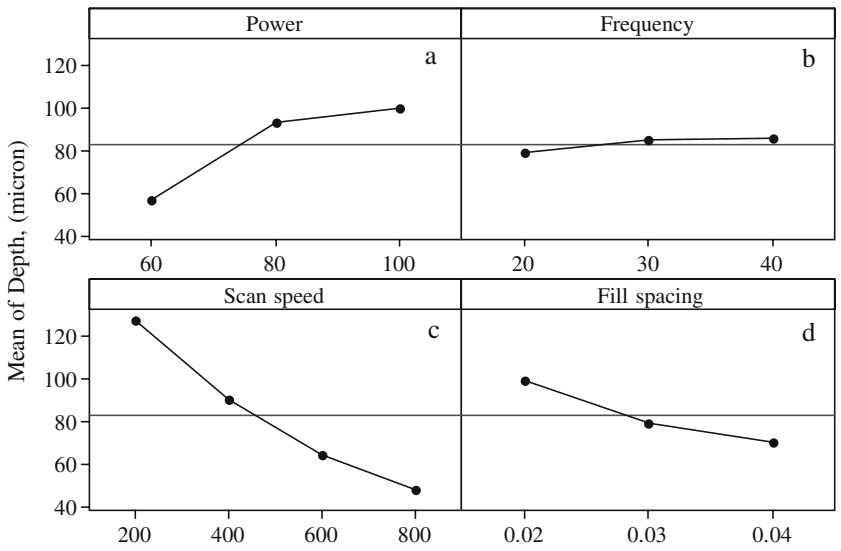

Fig. 7 Main effects plot based on the full factorial design for the means of Dm

Table 7 Table of estimated coefficients for SR

Predictor	SR			
	Coef	SE Coef	*T*	*P*
Constant	−13.8970	3.8721	−3.589	0.001
P	0.3858	0.0426	9.059	0.000
F	0.0397	0.0402	0.989	0.326
SS	0.0206	0.0066	3.138	0.002
FS	−45.3704	40.1516	−1.130	0.262
P×SS	−0.0005	0.0001	−5.829	0.000
S=2,951	R^2=78.3%	R^2(adj)=76.9%		

The test results indicate that the experimental and the calculated values are almost close in both test conditions. The highest and lowest deviation between the experimental measurement and the calculated value for the SR is 14.24% and 1.42%, respectively. The highest and lowest deviation between the experimental measurement and the calculated value for the Dm is 7.85% and 3.73%, respectively. These values indicate that the predicted regression models can be used to determine SR and Dm in the industrial application of laser micro-milling process.

4 Discussion

4.1 The effect of parameters on the surface roughness and milling depth

The hot work tool samples were machined by using a marker machine equipped with exit maximum power of 30W fiber laser. The experimental applications were conducted according to the process parameters given in Table 3, which composed of 108 different experiments. After milling process, the measured values of both SR and Dm were evaluated to determine the effects of the parameters used in the process.

Table 8 Table of estimated coefficients for Dm

Predictor	Dm			
	Coef	SE Coef	*T*	*P*
Constant	103.73	19.718	5.261	0.000
P	1.05	0.162	6.498	0.000
F	0.25	0.324	0.784	0.436
SS	−0.13	0.011	−12.172	0.000
FS	−1,540.15	324.167	−4.751	0.000
S=23.82	R^2=73.8%	R^2(adj)=72.4%		

Table 9 ANOVA table of the second-order regression model for SR based on the full factorial design

Source	DF	SS	MS	*F*	*P*
Regression	5	2,357.78	471.555	54.17	0.000
Linear	4	2,061.98	372.443	42.78	0.000
Interaction	1	295.80	295.800	33.98	0.000
Residual error	75	652.93	8.706		
Total	80	3,010.71			

In order to investigate the effect of process parameters on the SR and Dm, the graph of each parameter was plotted against the other parameters which were kept constant. Plots for SR and Dm under various test conditions are illustrated in Figs. 4 and 7, respectively.

4.1.1 Laser power

Figure 4a presents the relationship between the SR and the laser power. The results of experiments for laser power show that an increase in the scan speed yields decrease in the SR. The variation in the SR is between the values of 5 and 12 μm and also shows linearity. The 60% of the laser power was produced the lowest SR value for all combinations of parameters.

A similar trend was also observed for Dm. The Fig. 7a shows that any decrease in the laser power is caused to decrease in the Dm. The highest increase in the Dm is achieved between the laser power of 80% and 100%. The optimum values for the highest Dm are observed in when laser power of 100%.

4.1.2 Pulse frequency

The effect of pulse frequency on the SR is assessed in Fig. 4b. The plot shows that the SR decreases with a decrease in the frequency. Conversely, the Dm results indicate that as the frequency increases, the Dm increases which can be seen in Fig. 7b. Results for two outputs presented that optimum value for minimum SR is in 20 kHz while the maximum Dm is in 40 kHz.

Table 10 ANOVA table of the second-order regression model for Dm based on the full factorial design

Source	DF	SS	MS	F	P
Regression	4	121,200	30,300	53.40	0.000
Linear	4	121,200	30,300	53.40	0.000
Residual error	76	43,126	43,126		
Total	80	164,326			

Table 11 Results of confirmation tests for SR

Exp.	Power	Frequency	Scan speed	Fill spacing	Predicted values	Experimental values	Prediction error (%)
1	60	20	600	0.04	2.59	2.82	−8.8
2	100	40	600	0.02	7.72	7.43	3.75
3	80	30	600	0.02	5.61	5.53	1.42
4	60	30	600	0.03	3.44	3.93	−14.24

4.1.3 Scan speed

Figure 4c shows the relationship between the SR and the scan speed. According to experimental results, the SR decreases with an increase in the scan speed. The lowest average values are obtained at the scan speed of 800 mm/s. The lowest SR is measured as 1.75 μm when scan speed at 800 mm/s, power at 60%, frequency at 20 kHz, and fill spacing at 0.02 mm.

The curve for the scan speed indicates that the biggest variation in the SR is observed in between speed of 200 and 400 mm/s. An improvement of more than 250% with increasing the scan speed is achieved for SR and concluded that any increase in the scan speed tends to decrease in the SR.

The results of the Dm measurements are presented in the Fig. 7c. It is observed that the Dm becomes greater with the decrease in the scan speed. The highest average Dm is obtained at the scan speed of 200 mm/s. The curves for SR and Dm indicated that a linear relationship within the test value of the scan speed.

As it can be seen in both Figs. 4c and 7c, the SR and Dm decrease with increase in the scan speed. It is obvious that the scan speed creates opposite effect on the optimum value for outputs of milling experiments.

4.1.4 Fill spacing

Figures 4d and 7d present the relationship between the SR and Dm with fill spacing. Three values of fill spacing were selected to investigate its effect on the outputs. The graphics show that the fill spacing in 30 μm is produced better SR while the fill spacing in 20 μm is produced the highest Dm.

4.2 Combination of process parameters

The results of the laser milling experiments indicated that the scan speed and the power have great effect on the SR and Dm. Some scientific works in the related literature emphasizes that the percentage overlap affects the surface texture and machining depth. The overlap is the distance between two consecutive pulses in the same direction [5, 7, 10] which is depicted in Fig. 8. Combination of the scan speed and the frequency determine the percentage overlap rate which can be calculated by Eq. 3.

$$\begin{aligned} O_{\mathrm{p}} &= \frac{x}{D} = \left[1 - \frac{L}{D}\right] \times 100 \\ L &= \frac{SS}{F} \end{aligned} \tag{3}$$

where SS is the scan speed (mm/s), F is the frequency (kHz), D is the beam diameter (μm), x is the overlap length, and L is the center to center distance between the laser beam spots. Figure 9a and b represents an optical macrographs when scan speed "S"=2,000 mm/s, frequency "F"=20 kHz and S=4,000 mm/s, F=20 kHz, respectively. Results showed that the scan speed has great effect on the percentage overlap.

According to Eq. 3, the effect of the scan speed and frequency on the percentage overlap of consecutive pulses at the scan direction is depicted in Fig. 10. The beam diameter is measured and held constant at 100 μm for all experiments. When the frequency and beam diameter is

Table 12 Results of confirmation tests for Dm

Exp.	Power	Frequency	Scan speed	Fill spacing	Predicted values	Experimental values	Prediction error (%)
1	100	20	600	0.03	89.53	85.98	3.96
2	80	40	600	0.04	47.92	49.71	−3.73
3	100	30	600	0.02	107.43	99	7.85
4	60	20	600	0.03	47.53	45.10	5.11

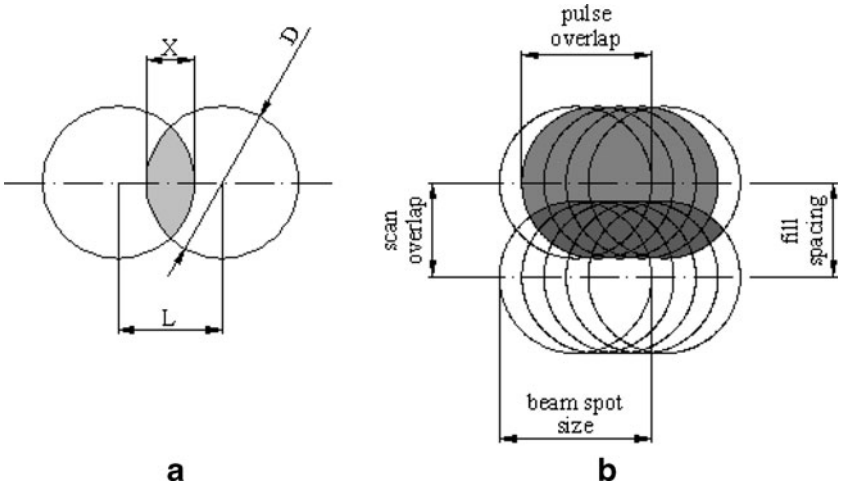

Fig. 8 Pulse overlap rate (**a**) and illustration of the scan overlap and pulse overlap (**b**)

held constant, an increase in the scan speed causes a decrease in the percentage overlap rate (Table 13).

The experimental results indicate that the scan speed and frequency together have a great effect on the percentage overlap. An increase in the scan speed and a decrease in the frequency reduce the percentage overlap. It is obvious that larger overlap increases the substrate temperature. If the consecutive pulses increase per unit area, the surface temperature will rise and the cooling will slow down. Thus, the surface temperature will continue to next pulse and it will rise with every laser pulse irradiating the same point [8]. This phenomenon creates higher SR and Dm.

The fill spacing defines the distance between two consecutive scan lines and is used to determine the scan overlap between scan lines. Figure 11 shows the scan overlap values for varying fill spacing. The low values of fill spacing corresponds the higher scan overlap. Higher scan overlap causes to increase in the energy per unit area and results in higher amount of removed material [5]. The experimental results show that lower fill spacing is produced higher milling depth due to the increase in the laser energy per unit area.

4.3 The effect of parameters on the energy density

It is clearly seen from the results that the power of 60% and the scan speed of 800 mm/s gives the lowest SR and Dm. This can be due to the lower energy density.

The SR and Dm depend on energy density, types of materials, and interaction time of the beam/material. Some scientific studies [11–13] related to the surface treatment by laser used Eqs. 3, 4, and 5 to calculate energy density and interaction time, respectively.

$$P_{\mathrm{d}} = \frac{P}{A}\left(\mathrm{W/mm^2}\right) \tag{4}$$

$$\tau = \frac{D}{SS}(\mathrm{s}) \tag{5}$$

$$E_{\mathrm{v}} = P_{\mathrm{d}} \cdot \tau(\mathrm{J/mm^2}) \quad \Rightarrow \quad E_{\mathrm{v}} = \frac{P \cdot D}{A \cdot SS} \tag{6}$$

Where E_{v} is the volume energy density (J/mm^2), P_{d} is the power density, P is the initial laser power (W), τ is the

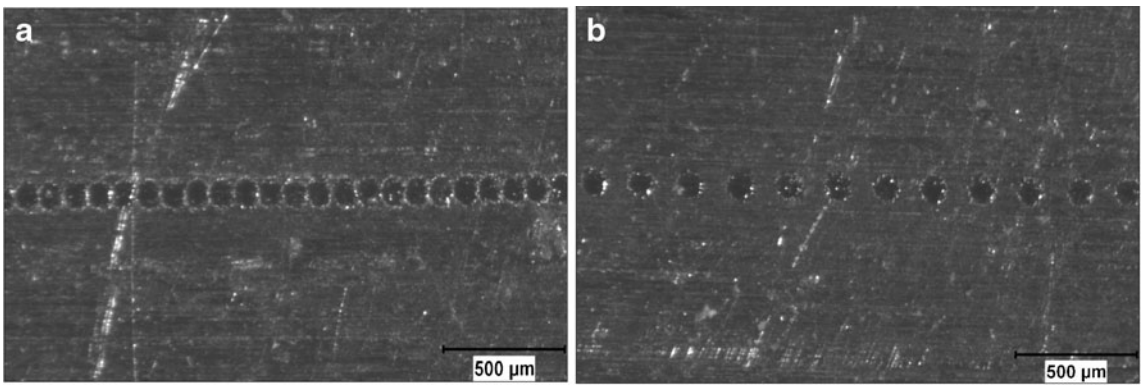

Fig. 9 The percentage overlap **a** S=2,000 mm/s, F=20 kHz; **b** S=4,000 mm/s, F=20 kHz

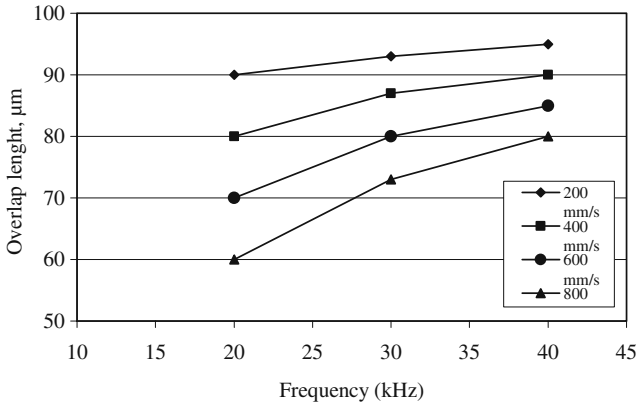

Fig. 10 The percentage overlaps as a function of frequency and scan speed

interaction time, A is the area, SS is the scan speed, and D is the beam diameter.

In this study, for all experiments, the material and the beam diameter were the same and thus, their effects on the outputs can be neglected. The effect of scan speed on SR is examined and showed that the scan speed has opposite effect compared with the laser power. The SR decreases with the increase of scan speed which can be explained by the interaction time between the laser beam and the material. This assumption which based on laser machining phenomenon is explained by energy density. According to Eq. 5, any decrease in the scan speed causes increase in interaction time. The amount of energy density per unit area may be expressed as in Eq. 6, depending on the formula, if the laser power held constant, the energy density per unit volume increases. The thickness of vaporized or removed layer is affected by the beam/material interaction time which determines the energy density and if the energy density is high enough, the vaporization mechanism occurs. The SR and Dm can be expressed in two cases:

1 Increase in the energy density increases heat input led to increase in the substrate temperature. Lower scan speed increases the interaction time. Consequently, higher interaction time and laser beam power increases energy density. When substrate temperature and heat input increase, the SR and Dm increase, but this effect is not linear. Thus, in order to produce minimum SR, the scan speed must be selected in the higher value, whereas to produce deeper cavities, the scan speed must be selected in the lower value.
2 The consecutive pulses determine the overlapping beam pulses. The larger overlap which signifies several consecutive laser beams irradiates per unit area. Larger overlap increases the heat input and the substrate temperature, which increases the SR and Dm of machined area.

Table 13 The overlap length (x, µm)

Scan speed (mm/s)	Frequency		
	20 kHz	30 kHz	40 kHz
200	90	93	95
400	80	87	90
600	70	80	85
800	60	73	80

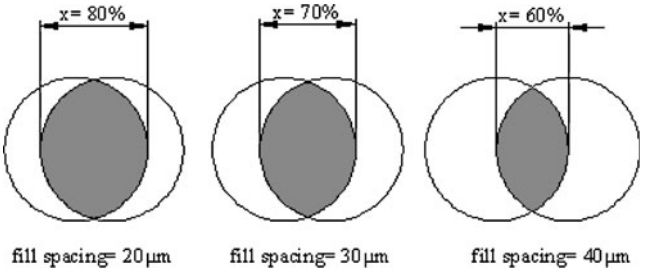

Fig. 11 Scan overlap values for varying fill spacing

In order to obtain better surface in the deep cavity, it is recommended that the scan speed and the number of scan repetition times should be increased.

5 Conclusion

The laser micro-milling experiments oriented to engraving have been performed on AISI H13 hot work tool steel. The results indicate following conclusions:

- The surface roughness and milling depth for all experiments significantly depends on laser scan speed and laser power. The decrease in the scan speed and laser power is corresponded by increase in energy input. Higher energy input is produced higher milling depth. The scan speed of 200 mm/s and laser power of 100% produced highest values of Dm. The value is 195 µm.
- The surface roughness decreases with decrease in the laser power and frequency when the surface is machined with high scan speed.
- The milling depth increased with the decrease of scan speed and fill spacing. However, a lower value of scan speed and fill spacing decreased the surface roughness.
- The optimum experimental condition for minimum surface roughness is the scan speed of 800 mm/s, laser power of 60%, frequency of 20 kHz, and fill spacing of 0.03 mm. However, the maximum milling depth is the scan speed of 200, laser power of 100%, frequency of

40 kHz, and fill spacing of 0.02 mm. The lowest SR obtained above condition is 1.75 μm. The highest Dm obtained above condition is 195 μm.

- The regression analysis-based prediction of SR and Dm are implemented and compared with the experimental value. The results for the SR showed that the main effects of laser power and scan speed are statistically significant at the 5% level. The results for the Dm showed that the main effects of laser power, scan speed, and spacing are statistically significant at the 5% level. The frequency was not any statistically significant at the 5% for both the SR and Dm.
- The predicted values obtained from regression model of both SR and Dm were close to the measured value of experimental tests. The highest prediction errors of the regression model were 14.24 and 7.85 for SR and Dm, respectively. The results of prediction error indicate that the regression models can be used to predict the surface roughness and milling depth.

Acknowledgments We are grateful to Laser Mikron Ltd.Sti. Company where the laser milling experiments were performed in Izmir, Turkey. This work was supported by Ege University under project no.35MUH08.

References

1. Kacar E, Mutlu M, Akman E, Demir A, Candan L, Canel T, Gunay V, Sınmazcelik T (2009) Characterization of the drilling alumina ceramic using Nd:YAG pulsed laser. J Mater Process Technol 209(Issue 4):2008–2014
2. Dubey AK, Yadava V (2008) Laser beam machining—a review. Int J Mach Tools Manuf 48:609–628
3. Leone C, Genna S, Caprino G, De Iorio I (2010) AISI 304 stainless steel marking by a Q-switched diode pumped Nd:YAG laser. J Mater Process Technol 210:1297–1303
4. Leone C, Lopresto V, De Iorio I (2009) Wood engraving by Q-switched diode-pumped frequency-doubled Nd:YAG green laser. Opt Lasers Eng 47(Issue 1):161–168
5. Yasa E, Kruth J-P (2010) Investigation of laser and parameters for selective laser erosion. Precis Eng 34(Issue 1):101–112
6. Cicala E, Soveja A, Sallamand P, Grevey D, Jouvard JM (2008) The application of the random balance method in laser machining of metals. J Mater Process Technol 196:393–40
7. Campanelli SL, Ludovico AD, Bonserio C, Cavalluzzi P, Cinquepalmi M (2007) Experimental analysis of the laser milling process parameters. J Mater Process Technol 191:220–223
8. Wendland J, Harrison PM, Henry M, Brownell M (2005) Deep engraving of metals for the automotive sector using high average power diyod pumped solid state lasers. International congress on application of lasers and electro-optics, Miami, October
9. Qi J, Wang KL, Zhu YM (2003) A study on the laser marking process of stainless steel. J Mater Process Technol 139:273–276
10. Kaldos A, Pieper HJ, Wolf E, Krause M (2004) Laser machining in die making—a modern rapid tooling process. J Mater Process Technol 155–156:1815–1820
11. Lee JH, Jang JH, Joo BD, Son YM, Moon YH (2009) Laser surface hardening of AISI H13 tool steel. Transection of Nonferrous Metals Society of China 19:917–920
12. Beal VE, Erasenthiran P, Hopkinson N, Dickens P, Ahrens CH (2006) Optimization of processing parameters in laser fused H13/Cu materials using response surface method (RSM). J Mater Process Technol 174:145–154
13. Stavrev DS, Dikova TSD, Shtarbakov VL, Milkov MP (2009) Laser surface melting of austenitic Cr-Ni stainless steel, The International Conference on Advances in Materials and Processing Technologies (Ampt 2009), Malaysia, October
14. Byeong-Don JOO, Jeong-Hwan JANG, Jae-Ho LEE, Young-Myung SON, Young-Hoon MOON (2009) Selective laser melting of Fe-Ni-Cr layer on AISI H13 tool steel. Trans Nonferrous Met Soc China 19:921–924
15. Haddad MJ, Fadaei Tehrani A (2008) Material removal rate (MRR) study in the cylindrical wire electrical discharge turning (CWEDT) process. J Mater Process Technol 199:369–378
16. Prakash O, Talat M, Hasan SH, Pandey RK (2008) Factorial design for the optimization of enzymatic detection of cadmium in aqueous solution using immobilized urease from vegetable waste. Bioresour Technol 99:7565–7572